Article

Journal of
Nanoscience and Nanotechnology
Vol. 16, 2847–2852, 2016
www.aspbs.com/jnn

Simultaneous Reduction of Vanadium (V) and Chromium (VI) in Wastewater by Nanosized $ZnWO_4$ Photocatalysis

Zengying Zhao[1,*], Baogang Zhang[2], Daimei Chen[1], Zhanhu Guo[3], and Zhijian Peng[4]

[1] *School of Science, China University of Geosciences, Beijing 100083, P. R. China*
[2] *School of Water Resources and Environment, China University of Geosciences, Beijing 100083, P. R. China*
[3] *Integrated Composites Laboratory (ICL), Dan F. Smith Department of Chemical Engineering, Lamar University, Beaumont, Texas 77710, United States*
[4] *School of Engineering and Technology, China University of Geosciences, Beijing 100083, P. R. China*

Vanadium (V, V) and chromium (Cr, VI) are simultaneously photocatalytically reduced to less-toxic V(VI) and Cr(III) by mimetic solar light with $ZnWO_4$ nanoparticles prepared by hydrothermal synthesis. The reduction efficiencies can reach 68.8% for V(V) and 97.3% for Cr(VI) in 3 h, respectively, which are comparable to those by microbial fuel cell technology carried out in over 10 days. The prepared $ZnWO_4$ nanoparticles are characterized by XRD, SEM, EDS, TEM, and Uv-vis-DRS tests. Electrochemical calculation shows high acidity benefits the rapid reduction of V(V) and Cr(VI). In addition, the applied $ZnWO_4$ nanoparticles can be recycled and reused for 5 repeated photocatalytic reduction runs. And after 5 runs, the recycled $ZnWO_4$ nanoparticles can also present good photocatalytic activity with a reduction efficiency of about 60% for V(V) and 90% for Cr(VI). The new procedure on the simultaneous reduction of V(V) and Cr(VI) by photocatalysis may be promisingly applied in contaminated wastewaters, combining the remediation and possible V and Cr recovery.

Keywords: Nanosized $ZnWO_4$, Photocatalysis, Vanadium, Chromium, Simultaneous Reduction, Wastewater Treatment.

1. INTRODUCTION

Combined pollutant in wastewaters is widely produced throughout the world, bringing serious challenges and constrains on conventional wastewater treatments.[1–3] Vanadium (V, V) and chromium (Cr, VI) are the main toxic and even fatal metals found in wastewater discharged from V mining.[4] They are often produced in large quantities in water with low pH value even to about 1.8 and concentrations usually from 10 to 400 mg/L.[5] And the toxicity of V depends on its chemical state, in which V(V) is more toxic than the other species of V.[6,7] Meanwhile, Cr(VI), identified as one of the 17 chemicals posing the greatest threat to human health, is a well-known mutagen, teratogen, and carcinogen, besides being highly corrosive.

Previous methods for the removal of V(V) from wastewater have been limited in the use of chemical precipitation and sorption.[8–10] As for the removal of Cr(VI), the methods have involved in the use of cationic and anionic ion-exchange resins, chemical and electrochemical precipitation, membrane filtration, and sorption.[11,12] These methods are usually operated with high cost, generating large amount of sludge that is difficult to be disposed. Besides, these methods can hardly recover the valuable metals from the treatment process. To date, few publications have been available that address the techniques for the removal and recovery of V(V) from V containing wastewater without generating sludge.[13] In our previous work, a microbial fuel cell technology (MFC) was reported to simultaneously reduce V(V) to V(IV) and Cr(VI) to Cr(III) from mining wastewater.[2] However, over 10 days was needed for one experiment turn with the highest reduction efficiency for V(V) of only 67.9%.

In literature, heterogeneous photocatalysis reduction (HPR), as a relatively new technique for water or air purification, can work under natural sunlight, which is an appealing opportunity for green chemistry.[14] For HPR,

*Author to whom correspondence should be addressed.

TiO_2 is the most widely investigated photocatalyst, exhibiting very good photocatalytic performance and stability in aqueous media under illumination. However, the applied TiO_2 suffers from low light conversion efficiency and wide band gap.[15, 16] On the other hand, transition metal tungstates of MWO_4 type (M = Co, Cu, Cd, Mn, Pb and Zn) are attracting more and more attention due to their interesting physicochemical properties, such as ferroelasticity, ionic conductivity, and photoluminescence.[17] Recently, the photocatalytic properties of MWO_4 toward the degradation of organic contaminants under UV and visible-light irradiation have been reported,[18–23] among which $ZnWO_4$ presents the highest photocatalytic activity in the degradation of methylene blue (MB) and methyl orange (MO).[24–26] Although the photocatalytic reduction of individual Cr(VI) has been investigated,[27–29] and there has paper about the individually photocatalytic reduction of V(V) has been published recently.[30] Until now, the simultaneously photocatalytic reduction of V(V) and Cr(VI) has not been reported, and further investigation is needed in order to bridge the existing gaps.

The conversion of V(V) and Cr(VI) to less toxic V(IV) and Cr(III) would be a useful approach for the remediation of contaminated water. Besides, the resultant V(IV) and Cr(III) can be easily precipitated and separated by controlled precipitation.[31–33] Apparently, from these considerations, photocatalytic reduction of V(V) and Cr(VI) simultaneously from wastewater is of significant importance. In the present study, a new technique is reported, i.e., V(V) and Cr(VI) are simultaneously reduced to the less toxic V(IV) and Cr(III) both in a rather high reduction efficiency by homemade $ZnWO_4$ nanoparticles using a photocatalytic method.

2. EXPERIMENTAL DETAILS

2.1. Synthesis of Nanosized $ZnWO_4$ Particles

All chemicals used in the present experiments were obtained from commercial sources, and were analytic grade reagents without any further purification. The applied nanosized $ZnWO_4$ was synthesized by a hydrothermal method. In a typical synthesis, it started from the stoichiometric amounts of $Zn(NO_3)_2 \cdot 6H_2O$ and $Na_2WO_4 \cdot 2H_2O$. And the following procedure was accomplished at room temperature: two transparent solutions were obtained by dissolving 1×10^{-3} mol of $Zn(NO_3)_2 \cdot 6H_2O$ in 30 mL of distilled water (solution A) and 1×10^{-3} mol of $Na_2WO_4 \cdot 2H_2O$ in 30 mL of distilled water (solution B), respectively. Afterwards, the solution A was added dropwise to solution B under vigorous stirring. The pH value of the mixed solution was then adjusted to 9.0 using dilute H_2SO_4 and NaOH solution (0.5 M). After being vigorously stirred for about 30 min, the solution was loaded into a 100 mL teflon-lined autoclave. The autoclave was then heated to 180 °C and maintained at this temperature for 24 h under autogenous pressure and then cooled down to room temperature naturally. The white precipitate was collected and washed with distilled water and ethanol for several times. Finally, the sample was dried in a vacuum oven at 50 °C for 4 h.[34]

2.2. Product Characterization

The phase composition of the products was identified by powder X-ray diffraction (XRD) on a Bruker D8-Advance X-ray diffractometer at 40 kV and 100 mA with Cu Kα radiation ($\lambda = 1.5406$ Å) through a continuous scanning mode at a speed of 5°/min. The microstructure of the products was examined by a JSM-6390LV scanning electron microscope (SEM), which was attached with an energy dispersive X-ray (EDX) spectroscopy, and a JEM2010 transmission electron microscope (TEM). The UV–vis absorption spectra were recorded on a Varian Cary 100 Scan UV–vis system equipped with a lab sphere diffuse reflectance accessory.

2.3. Photocatalytic Reduction of V(V) and Cr(VI)

The UV-light photocatalytic reduction of V(V) and Cr(VI) was carried out in a cylindrical pyrex flask with a capacity of 100 mL. Typically, the reaction system containing 50 mL V(V) and Cr(VI) aqueous solution (both in 10 mg/L) and $ZnWO_4$ nanoparticles (50 mg) was first magnetically stirred under a dark cover for 30 min to reach the adsorption equilibrium of metal ions with the catalyst, and then exposed to the light from a 500 W Hg lamp equipped with a cutoff filter (313 nm $< \lambda <$ 400 nm). The Hg lamp has the strongest emission at 365 nm. At specific time intervals, 3 mL of the reactive solution was taken from the reaction system by a syringe. Then the collected solution was centrifuged to remove the $ZnWO_4$ powder. After that, the amounts of V(V) and Cr(VI) were analyzed by the spectrophotometric method at 540 and 600 nm, respectively.[5] And the reduction efficiency for V(V) was determined as the ratio of the V(V) concentration before and after the catalytic reaction, so as the reduction efficiency of Cr(VI).

3. RESULTS AND DISCUSSION

3.1. Phase Composition Analysis of the Product

Figure 1 shows the XRD patterns of the as-prepared $ZnWO_4$ powder. The measured lattice constants are $a = 4.691$, $b = 5.720$, and $c = 4.925$ Å, and all the detected diffraction peaks can be well indexed to pure monoclinic sanmartinite $ZnWO_4$ (JCPDS card no. 15-0774) without detecting any other impurities, suggesting the successful preparation of $ZnWO_4$ crystals.[25] The calculated particle size of the prepared $ZnWO_4$ powder by Scherrer equation using the parameters of (002) peak is 122 nm. In addition, the XRD pattern of the product presents the peaks of a sharp shape in Figure 1, indicating the leading role of hydrothermal treatment in improving the crystallization of $ZnWO_4$.[35]

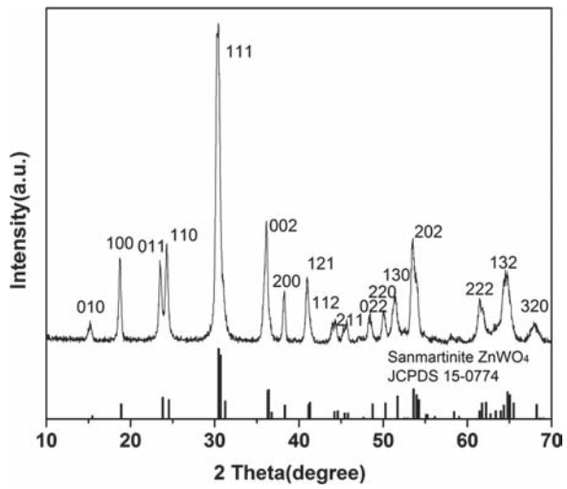

Figure 1. Typical XRD pattern of the as-prepared $ZnWO_4$ powder.

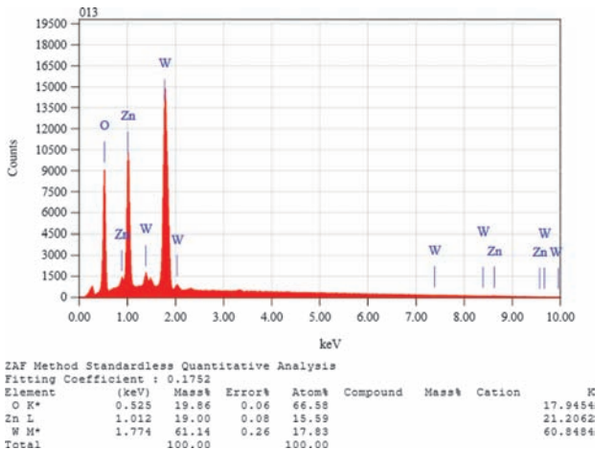

Figure 3. EDX spectrum of the as-prepared $ZnWO_4$ powder taken from the square as shown in Figure 2.

3.2. Microstructural Analysis on the Product

Figure 2 displays the typical SEM image of the as-prepared $ZnWO_4$ powder. The $ZnWO_4$ photocatalyst was presented as homogeneous particles. The recorded EDX spectrum shows that the prepared photocatalyst almost has the same stoichiometry with pure $ZnWO_4$ (Fig. 3). It is also clearly observed from Figure 4(a) that the $ZnWO_4$ nanoparticles are of homogeneous morphology with a particle size of about 100 nm, which is in accordance with the calculated result by the Scherrer equation from XRD analysis. The $ZnWO_4$ product is rod-like particles, and each particle is 100 nm in length and 30 nm in width. Besides, Figure 4(b) shows the high-resolution field-emission TEM (HRTEM) image of $ZnWO_4$ nanoparticles. The lattice fringe spacing is 0.566 nm, which corresponds well to the characteristic (010) planes of $ZnWO_4$.

3.3. UV-Vis Diffuse Reflectance Spectrum of the Product

The optical properties of $ZnWO_4$ particles are very essential for determining their photocatalytic efficiency. Figure 5 illustrates a typical UV-vis-diffuse reflectance spectrum (DRS) of the as-prepared $ZnWO_4$ nanoparticles. The absorption intensity was observed to be mainly in the range of ultraviolet, as reported in Ref. [36]. The observed steep shape of the spectrum indicates that the UV light absorption is due to the band-gap transition instead of the

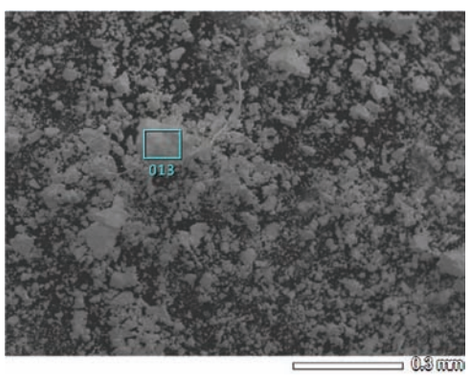

Figure 2. Typical SEM image taken on the as-prepared $ZnWO_4$ powder.

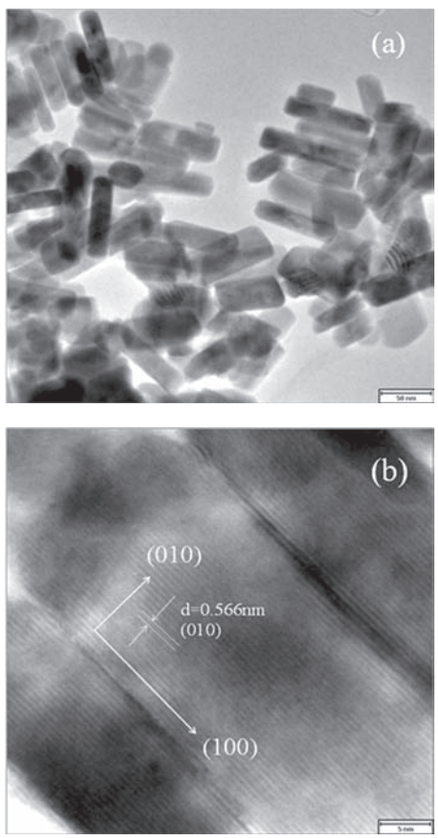

Figure 4. TEM (a) and HRTEM (b) images of the as-prepared $ZnWO_4$ powders.

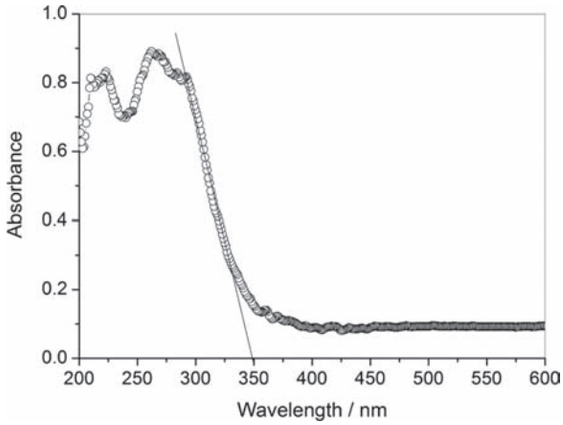

Figure 5. Typical diffuse reflectance absorption spectrum of the as-prepared $ZnWO_4$ powder.

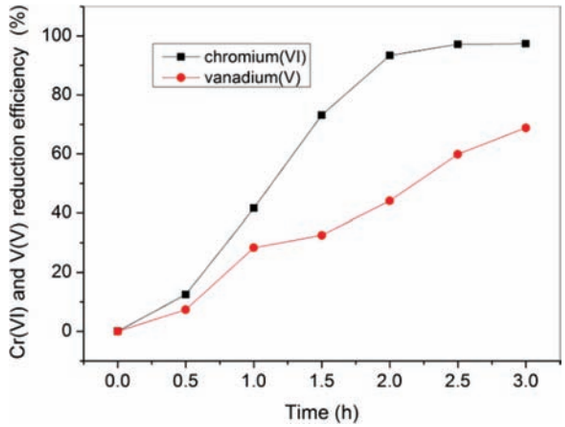

Figure 6. Photocatalytic reduction efficiency of V(V) and Cr(VI) by the as-prepared nanosized $ZnWO_4$ particles.

transition from the impurity level. Two peaks appeared in the range of 200–350 nm for the sample. The peaks at 292 and 262 nm could be attributed to direct excitation in $ZnWO_4$, while the peak at 219 nm was correlated to the electron transfer from the anion to the cation sublattice.[37] For a crystalline semiconductor, the optical absorption near the band edge, E_g, follows the equation: $E_g = 1240/\lambda$, wherein λ is the wavelength obtained from the tangent line of the UV-vis-DRS of $ZnWO_4$. By the equation, E_g was calculated to be 3.54 ev. The band gap energies of $ZnWO_4$ photocatalysts were coincident with the literature.[38, 39] For *W*-based semiconductors, it was already found that excitons are formed due to the transitions into the tungstate W_{5d} states hybridized with O_{2p} and possess a very strong tendency for self-trapping. Free electrons and holes can be created due to the transitions into cationic states.[40] An active photocatalyst for the reduction of high valence metal ions must have a conduction band (CB) with strong reducing ability and photogenerated electrons with high mobility. The CB of $ZnWO_4$ has shown strong ability to photocatalytic reduction of the high valence metal ions in the work described in the next section.

3.4. Photocatalytic Reduction of V(V) and Cr(VI) by Nanosized $ZnWO_4$ Particles

The photocatalytic activities of the prepared $ZnWO_4$ nanoparicles for the reduction of V(V) and Cr(VI) are shown in Figure 6. The reduction efficiencies for V(V) and Cr(VI) were 68.8% and 97.7%, respectively, after 180 min of irradiation. However, it will take 10 days to get the same reduction efficiencies by MFC technology.[5]

From Figure 6, it can be seen that the reduction efficiency of Cr(VI) increased rapidly at the beginning and became stable after 2 h of radiation, while the reduction efficiency for V(V) increases steadily during the whole 3 h operating period. And the reduction efficiency of V(V) is comparable to that of our previous work, in which the reaction was operated for ten days with a reduction efficiency of V(V) of 67.9%.[5] From Figure 6, it can also be seen that Cr(VI) is reduced more quickly than V(V). Although both V(V) and Cr(VI) have high electrochemical redox potentials as presented in Eqs. (1) and (2), the electrochemical redox potential of Cr(VI) was relatively higher than that of V(V). So electrons from anode are first consumed by Cr(VI) reduction.

$$VO^{2+} + 2H^+ + e^- \rightarrow VO^{2+} + H_2O \qquad E^\Theta = 0.991\ \text{V} \quad (1)$$

$$Cr_2O_7^{2-} + 14H^+ + 6e^- \rightarrow 2Cr^{3+} + 7H_2O \qquad E^\Theta = 1.33\ \text{V} \quad (2)$$

If we suppose that at the begining there are 0.1% of V(V) and Cr(VI) reduced to V(IV) and Cr(III), after 3 h of photocatalysis reaction, according to Figure 6, there will be actually 68.8% of V(V) reduced to V(IV), and 97.3% of Cr(VI) be reduced to Cr(III), respectively. From Nernst equation, from the beginning to the end of the reaction, the actual potentials (mV) of both V and Cr redox reactions are presented as follows:

$$E_{Cr} = 1330 - 138.1 \times \text{pH} - 9.862 \times \lg[Cr^{3+}]^2/[Cr_2O_7^{2-}] = 1140 \sim 1078\ \text{mV} \quad (3)$$

$$E_V = 991.0 - 118.4 \times \text{pH} - 59.17 \times \lg[VO^{2+}]/[VO_2^+] = 955.5 \sim 756.2\ \text{mV} \quad (4)$$

where $[VO^{2+}]$, $[VO^{2+}]$, $[Cr^{3+}]$ and $[Cr_2O_7^{2-}]$ are the concentrations of the different types of ions in the solution. Thus the electrons can be transferred to Cr(VI) more conveniently. The E_{Cr} and E_V values increased with the increasing concentration of H^+, indicating the higher ability of accepting electrons of Cr(VI) at lower pH. In addition, Cr(III) would be precipitated on the surface of photocatalysts as $Cr(OH)_3$ at increased solution pH, covering the activity sites of the catalysts.[41] And V(IV) would be precipitated in the form of VOX_2 (X^- is anions).[42]

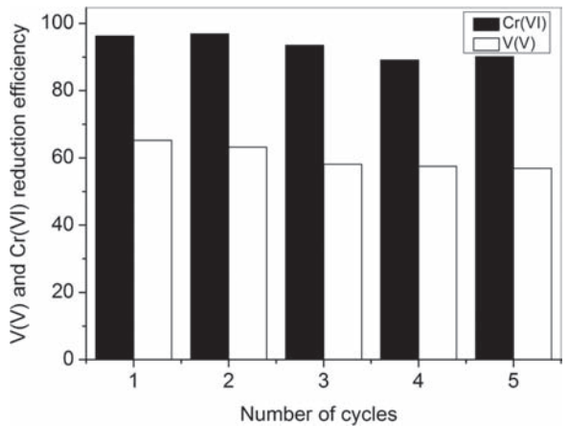

Figure 7. Photocatalytic reduction efficiency of V(V) and Cr(VI) with repeated use of nanosized $ZnWO_4$ in 5 consecutive cycles.

Therefore, this better performance could be attributed to the relatively higher actual electrochemical redox potentials of Cr(VI) and V(V) and the activity sites of the catalysts at low pH in this work.

3.5. Durability of the Nanosized $ZnWO_4$ Particle Photocatalyst

To determine the durability and reusability of the prepared $ZnWO_4$ nanoparticles, the photocatalyst was separated from the aqueous solution after each reaction run, followed by washing with distilled water and ethanol for several times. Then the sample was dried in a vacuum oven at 50° for 4 h. Afterwards, the photocatalyst was re-used in the subsequent reaction under identical conditions. The result is presented in Figure 7. As seen from this figure, the photocatalytic reduction efficiencies of V(V) and Cr(Cr) remained fairly consistent throughout the 5 repetitive experiments. This result reveals that the photocatalyst continues to reduce high valence metal ions after each reduction cycle, with a stable reduction efficiency of around 60% for V(V) and 90% for Cr(VI). Hence, the as-prepared $ZnWO_4$ particles exhibited great potential for repeated utilization in the photocatalytic reduction of V(V) and Cr(VI).

As previously mentioned, V(V) is the most toxic of the species of V, after the reduction of V(V) to V(IV), the element becomes less toxic and can be easily treated by downstream processes.[2] At present, the conventional method to treat Cr(VI) is to reduce it by chemical or biological means into non-toxic Cr(III). The HPR technology presented here can simultaneously reduce V(V) and Cr(VI) in a very short time compared with biological mean and without sludge compared with chemical wastewater treatment.

4. SUMMARY

V(V) and Cr(VI) are pollutants commonly found in V mining wastewater. By employing V containing wastewater as the photogenerated electrons acceptor, the simultaneous reduction of V(V) and Cr(VI) has been successfully achieved by using nanosized $ZnWO_4$ as photocatalyst. The maximum photocatalytic reduction efficiencies reach 68.8% for V(V) and 97.3% for Cr(VI) in 3 h, which is a relatively short time when compared with biological treatment method. The high acidity of the V mining wastewater benefits the rapid reduction of V(V) and Cr(VI). After 5 repeated reduction runs, the recycled $ZnWO_4$ still showed good photocatalytical reduction activity. The result shows that the photocatalyst used in the present study has good durability and bright prospect of practical applications.

Acknowledgment: This work was financially supported by "the Fundamental Research Funds for the Central Universities of China, No. 2652013107," and the Laboratory Open Funds of China University of Geosciences (Beijing), No. 2014BXZ021.

References and Notes

1. J. Zhang, B. Zhang, C. Tian, Z. Ye, Y. Liu, and Z. Lei, *Bioresour Technol.* 138, 198 (**2013**).
2. V. I. Starostin, O. G. Sorokhtin, *Geosci. Front* 2, 583 (**2011**).
3. G. Velvizhi and S. V. Mohan, *Bioresour Technol.* 102, 10784 (**2011**).
4. W. Carpentier, K. Sandra, I. Smet, A. Brigé, L. D. Smet, and J. V. Beeumen, *Appl. Environ. Microbiol.* 69, 3636 (**2003**).
5. B. G. Zhang, H. Z. Zhao, C. H. Shi, S. G. Zhou, and J. R. Ni, *J. Chem. Technol. Biotechnol.* 84, 1780 (**2009**).
6. A. Safavi, M. R. H. Nezhad, and E. Shams, *Ana. Chim. Acta* 409, 283 (**2000**).
7. K. Pyrzyńska and T. Wierzbicki, *Talanta* 64, 823 (**2004**).
8. F. Kaczala, M. Marques, and W. Hogland, *Bioresour Technol.* 100, 235 (**2009**).
9. A. Bhatnagar, A. K. Minocha, and D. Pudasainee, *Chem. Eng. J* 144, 197 (**2008**).
10. W. De los Santos Ramos, T. Poznyak, and I. Chairez, *J. Hazard Mater.* 169, 428 (**2009**).
11. R. Khosravi, M. Fazlzadehdavil, and B. Barikbin, *Appl. Surf. Sci.* 292, 670 (**2014**).
12. M. Bansal, D. Singh, and V. K. Garg, *J. Hazard Mater.* 171, 83 (**2009**).
13. B. Zhang, S. Zhou, H. Zhao, C. Shi, L. Kong, J. Sun, Y. Yang, and J. Ni, *Bioprocess Biosys. Eng.* 33, 187 (**2010**).
14. S. Michela, R. Elisa, and M. Federica, *J. Hazard Mater.* 254, 179 (**2013**).
15. Z. B. Zhang, C. C. Wang, and R. Zakaria, *J. Phys. Chem. B* 102, 10871 (**1998**).
16. Y. C. Miao, Z. B. Zhai, and L. Jiang, *Powder Technol.* 266, 365 (**2014**).
17. U. M. Garcia-Perez, A. Martinez-de la Cruz, and J. Peral, *Electrochim Acta* 81, 227 (**2012**).
18. Z. Shan, Y. Wang, H. Ding, and F. Huang, *J. Mol. Catal A* 302, 54 (**2009**).
19. H. Fu, C. Pan, L. Zhang, and Y. Zhu, *Mater. Res. Bull.* 42, 696 (**2007**).
20. T. Dong, Z. Li, Z. Ding, L. Wu, X. Wang, and X. Fu, *Mater. Res. Bull.* 43, 1694 (**2008**).
21. D. Ye, D. Li, W. Zhang, M. Sun, Y. Hu, Y. Zhang, and X. Fu, *J. Phys. Chem. C* 112, 17351 (**2008**).
22. H. Abdessalem, M. Noomen, and D. P. Agatino, *Appl. Catal. B-Environ.* 154, 379 (**2014**).
23. Y. Liu, M. Y. Zhang, and L. Li, *Appl. Catal. B-Environ.* 160, 757 (**2014**).

24. T. Montini, V. Gombac, A. Hameed, L. Felisari, G. Adami, and P. Fornasiero, *Chem. Phys. Lett.* 498, 113 (**2010**).
25. K. M. Garadkar, L. A. Ghule, K. B. Sapnar, and S. D. Dhole, *Mater. Res. Bull.* 48, 1105 (**2013**).
26. T. D. Savic, I. L. Validzic, and T. B. Novakovic, *J. Cluster Sci.* 24, 679 (**2013**).
27. H. Hsu, S. Chen, and Y. Chen, *Sep. Purif. Technol.* 80, 663 (**2011**).
28. J. Yang and S. Lee, *Chemosphere* 63, 1677 (**2006**).
29. J. Yang, J. Dai, and J. Li, *Environ. Sci. Pollut. Res.* 20, 2435 (**2013**).
30. M. Sturini, E. Rivagli, F. Maraschi, A. Speltini, and A. Profumo, *J. Hazard Mater.* 254, 179 (**2013**).
31. G. Chu, Z. A. Zhou, and T. Z. Yang, *Min Metall Eng.* 31, 69 (**2011**).
32. F. Rahman and M. Skyllas-Kazacos, *J. Power Sources* 72, 105 (**1998**).
33. D. M. Manohar, B. F. Noeline, and T. S. Anirudhan, *Ind. Eng. Chem. Res.* 44, 6676 (**2005**).
34. S. Lin, J. B. Chen, X. Weng, L. Yang, and X. Chen, *Mater. Res. Bull.* 44, 1102 (**2009**).
35. S. Chen, S. Sun, H. Sun, W. Fan, X. Zhao, and X. Sun, *J. Phys. Chem. C* 114, 7680 (**2010**).
36. Q. Zhang, X. Chen, and Y. Zhou, *J. Phys. Chem. C* 111, 3927 (**2007**).
37. V. Nagirnyi, E. Feldbach, L. Jönsson, M. Kirm, A. Kotlov, A. Lushchik, V. A. Nefedov, and B. I. Zadneprovski, *Nucl. Instrum. Methods A* 486, 395 (**2002**).
38. J. Lin, J. Lin, and Y. F. Zhu, *Inorg. Chem.* 46, 8372 (**2007**).
39. X. Zhao, W. Q. Yao, Y. Wu, S. C. Zhang, H. P. Yang, and Y. F. Zhu, *J. Solid State Chem.* 179, 2562 (**2006**).
40. G. L. Huang and Y. F. Zhu, *Mater. Sci. Eng. B* 139, 201 (**2007**).
41. S. R. Zheng, Z. Y. Xu, and Y. D. Wang, *J. Photochem. Photobiol. A* 137, 185 (**2000**).
42. P. Zhou, G. Xin, and C. Meng, Inorganic Chemistry, 5th edn., Higher Education Publishing, Beijing, China (**2012**).

Received: 17 October 2014. Accepted: 29 December 2014.